BIOCHEMISTRY
including biophysical chemistry & molecular biology
Article

Biochemistry **2010,** *49,* 1199–1206 1199
DOI: 10.1021/bi9018576

Determination of Separate Inhibitor and Substrate Binding Sites in the Dehaloperoxidase−Hemoglobin from *Amphitrite ornata*[†,‡]

Michael F. Davis,[§,#] Benjamin G. Bobay,[∥,⊥] and Stefan Franzen*[,§]

[§]*Departments of Chemistry, and* [∥]*Molecular and Structural Biochemistry, North Carolina State University, Raleigh, North Carolina 27606, and* [⊥]*North Carolina Research Campus, Kannapolis, North Carolina 28081.* [#]*Present address: Lineberger Comprehensive Cancer Center and Department of Biochemistry and Biophysics, University of North Carolina, Chapel Hill, NC 27599.*

Received October 29, 2009; Revised Manuscript Received January 11, 2010

ABSTRACT: Dehaloperoxidase−hemoglobin (DHP A) is a dual function protein found in the terrebellid polychaete *Amphitrite ornata*. *A. ornata* is an annelid, which inhabits estuary mudflats with other polychaetes that secrete a range of toxic brominated phenols. DHP A is capable of binding and oxidatively dehalogenating some of these compounds. DHP A possesses the ability to bind halophenols in a distinct, internal distal binding pocket. Since its discovery, the distal binding pocket has been reported as the sole binding location for halophenols; however, data herein suggest a distinction between inhibitor (monohalogenated phenol) and substrate (trihalogenated phenol) binding locations. Backbone $^{13}C\alpha$, $^{13}C\beta$, carbonyl ^{13}C, amide ^{1}H, and amide ^{15}N resonance assignments have been made, and various halophenols were titrated into the protein. $^{1}H-^{15}N$ HSQC experiments were collected at stoichiometric intervals during each titration, and binding locations specific for mono- and trihalogenated phenols have been identified. Titration of monohalogenated phenol induced primary changes around the distal binding pocket, while introduction of trihalogenated phenols created alterations of the distal histidine and the local area surrounding W120, a structural region that corresponds to a possible dimer interface region recently observed in X-ray crystal structures of DHP A.

The dehaloperoxidase−hemoglobin (DHP A)[1] is a globin with peroxidase activity found in the terebellid polychaete *Amphitrite ornata*. DHP A is one of two known proteins in *A. ornata* which contain the globin fold. Two isoforms of the dehaloperoxidase−hemoglobin are found in *A. ornata*, DHP A and DHP B (*1*). DHP B differs from DHP A by only five mutations (I9L, R32K, Y34N, N81S, and S91G) and has recently been cloned and expressed in *Escherichia coli* (*2*, *3*). Even though DHP A and DHP B are structurally homologous to typical myoglobins (Mbs) (*4*−*6*), DHP A was first isolated from *A. ornata* and characterized as a peroxidase (*7*). DHP A was later cloned into *E. coli*, expressed, and characterized as a function of pH (*8*, *9*). Site-directed mutations of the distal and proximal histidines, H55 and H89, respectively, have shown their essential nature in the catalytic mechanism of DHP A (*10*).

It has been known for more than a decade that DHP A has a unique ability to bind halogenated phenols in a distal pocket above the heme plane (*6*, *11*−*14*). We have recently demonstrated this internal binding site to be an inhibitor binding site favored by 4-halophenols, while the most active substrates, 2,4,6-trihalophenols, bind to an external active site (*13*, *15*). In addition to inhibition of peroxidase activity, a bound 4-halophenol in the distal cavity appears to interfere with the inherent role of globins in oxygen transport and NO scavenging (*11*, *12*, *15*, *16*). The role of 2,4,6-trihalophenol substrate binding is even more elusive since it is not directly observed in the X-ray crystal structure. Thus, there is a need for solution studies of both substrate and inhibitor binding to clarify the structural consequences of each binding event with DHP A.

A. ornata coinhabits estuary mudflats with other filter feeding marine polychaetes that secrete halophenols presumably for territorial protection (*17*−*19*). One of the coinhabitants, *Notomastus lobatus*, produces and excretes 4-bromophenol (4-BP), 2,4-dibromophenol (2,4-DBP), and 2,4,6-tribromophenol (2,4,6-TBP) to the surrounding sediment with a stoichiometric ratio of 1.8:0.9:1.0 (*20*). Brominated phenols are extremely toxic, particularly for aquatic organisms. The ability of DHP A to bind and oxidatively dehalogenate halophenols may therefore play an important role in the survival of *A. ornata*. Despite the globin fold, DHP A readily oxidizes various trihalogenated phenols, as illustrated in Scheme 1, with a total yield similar to that of horseradish peroxidase (HRP) (*8*−*10*, *21*). The oxidation rate, however, is ∼13 times less than HRP at pH 5 (*8*). Since HRP is a secretory peroxidase, it is optimized to function at pH 5. On the other hand, DHP A is optimized to function at pH 7.5, which is near the pH of cytosol. This value is consistent with the role of DHP A as a coelomic hemoglobin.

The internal binding pocket was initially thought to be the active site of DHP A, which was a reasonable assumption in the absence of detailed kinetic data and a structure of the external binding site (*6*). While the reactivity of DHP A toward

[†]This project was supported by Army Research Office Grant 52278-LS.

[‡]The DHPCN A magnetic coordinates have been deposited in the Biological Magnetic Resonance Data Bank (accession number 16401).

*To whom correspondence should be addressed. Phone: 919-515-8915. Fax: 919-515-8920. E-mail: Stefan_Franzen@ncsu.edu.

[1]Abbreviations: 4-BP, 4-bromophenol; 2,4,6-TBP, 2,4,6-tribromophenol; 2,4,6-TCP, 2,4,6-trichlorophenol; 2,4,6-TFP, 2,4,6-trifluorophenol; 2,6-DCQ, 2,6-dichloroquinone; Amp, ampicillin; CcP, cytochrome *c* peroxidase; DHP A, dehaloperoxidase−hemoglobin; DHPCN A, metcyano dehaloperoxidase−hemoglobin; HSQC, heteronuclear single-quantum coherence; HRP, horseradish peroxidase; IPTG, isopropyl β-D-thiogalactopyranoside.

Published on Web 01/12/2010

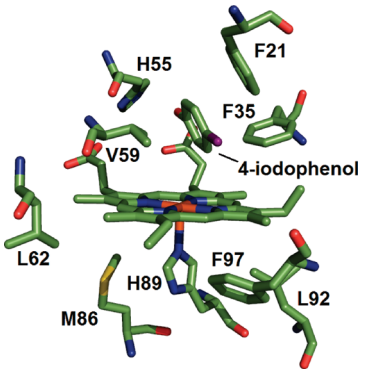

FIGURE 1: X-ray structure of the internal binding pocket of DHP A. The 1EWA X-ray structure illustrates binding of monohalogenated 4-IP in the distal pocket (*14*). The closest residues to bound 4-IP are F35, V59, and F21, respectively.

Scheme 1: DHP A Catalyzes the Oxidative Dehalogenation of Trihalophenol to the Corresponding Dihalogenated Quinone Product in the Presence of H_2O_2[a]

[a]The scheme represents the reaction at pH 6 where the substrate is in the phenol form.

2,4,6-trihalophenols is common in many peroxidases, the internal inhibitor binding pocket separates DHP A from any known globin or peroxidase. In fact, many of our early papers were based on this assumption that the internal binding pocket was the true substrate binding site. This led to a great deal of speculation about whether a one-electron or two-electron oxidation takes place in DHP A (*8*, *9*). However, the realization that an external site is the substrate binding site makes DHP A similar to other peroxidases and strongly suggests a one-electron oxidation mechanism. Inhibition of peroxidase activity, due to inhibitor binding in the distal pocket, is attributable to two main factors. The X-ray structure shown in Figure 1 illustrates bound 4-halophenol in the distal pocket (*14*). The close binding proximity of the inhibitor to the heme iron impedes access of H_2O_2 to the heme iron. H_2O_2 access is essential for formation of compound ES and subsequent peroxidase activity of the protein (*22*). Consequently, the steric interference of 4-halophenols provides one mechanism for inhibition. Second, the distal histidine is forced into a solvent-exposed position by the inhibitor. This conformational change results in DHP A inhibition because the distal histidine is the acid−base catalyst required for formation of the active compound ES.

At present, one of the major questions in DHP A function regards the structure of the true substrate binding site. Substrate binding is not observed in any of the X-ray crystal structures. While we can observe the binding of 4-iodo-, 4-bromo-, 4-chloro-, and 4-fluorophenol in the distal pocket, attempts to infuse 2,4,6-trihalophenols into crystals have not resulted in observed binding in a single X-ray crystal structure (*15*). We have treated the crystals with saturated solutions of 2,4,6-trihalophenols (substrates) exactly as we have done for 4-halophenols (inhibitors). Consequently, we turn to solution studies of DHP A in order to determine the conformation of the protein in response to substrate binding. The low water solubility of 2,4,6-trihalogenated phenols and apparent high K_D values make them poor choices for structural studies such as X-ray crystallography or NMR experiments. Of the active 2,4,6-trihalophenols only 2,4,6-trifluorophenol (2,4,6-TFP) and 2,4,6-trichlorophenol (2,4,6-TCP) have solubility greater than micromolar concentrations. 2,4,6-TCP is the closest analogue to the native substrate 2,4,6-TBP and is the best laboratory substrate due to its similar size and turnover rates. The most soluble trihalophenol, 2,4,6-TFP, has been used in cryogenic FT-IR, EPR, and HYSCORE studies to show binding at cryogenic temperature (< 260 K) but not at room temperature (*12*, *23*). Above 260 K the 2,4,6-TFP substrate leaves the distal binding pocket, and no other internal perturbations are observed (*12*). ^{19}F NMR and relaxation experiments provided initial evidence of an exterior binding site for 2,4,6-TFP at ambient temperatures (*13*). However, the exact location of 2,4,6-TFP binding has not been reported. Moreover, the use of 2,4,6-TFP as a substrate analogue may be a poor choice due to the relative size difference between fluorine and bromine or chlorine substituents.

In this report, assignments of the backbone $^{13}C\alpha$, $^{13}C\beta$, carbonyl ^{13}C, amide ^{1}H ,and amide ^{15}N resonances have been made using $^{13}C/^{15}N$ labeling and 3D NMR techniques. Paramagnetic low-spin metcyano DHP A was used in order to retain continuity with previous NMR investigations. Assignment of 92% of the backbone resonances allowed for observations of structural changes occurring throughout the protein upon introduction of various substrates or inhibitors. Titrations of inhibitor 4-BP and substrates 2,4,6-TCP/2,4,6-TFP were performed and monitored using $^{1}H-^{15}N$ HSQC experiments. Chemical shift deviations of backbone amide protons were observed for each substrate/inhibitor. The resonances exhibiting the greatest degree of change were then mapped onto current X-ray structures of the protein, and the local regions experiencing the largest deviations were analyzed.

MATERIALS AND METHODS

Protein Expression and Purification. The highly expressing His-DHP A 4R gene was inserted into the pET-16b vector and transformed into Rosetta (DE3) *E. coli* cells. The Rosetta cells were used for their slower growth cycle and additional chloramphenicol (Cam) resistance, not to supply tRNAs for poorly expressed *E. coli* codons. The cells were plated onto LB agar plates containing 100 μg/mL Amp and 34 μg/mL Cam and allowed to grow for ~18 h. Single colonies were isolated, and 2 mL starter growths in LB broth (100 μg/mL Amp, 34 μg/mL Cam) were allowed to grow at 37 °C overnight. One milliliter of the starter growth was then added to 1 L of Spectra 9-CN (Spectra Stable Isotopes, Inc.) medium with >98% ^{13}C and ^{15}N isotopes in the aforementioned Amp and Cam concentrations. The 1 L double-labeled growth was allowed to grow at 37 °C with shaking until an OD_{600} of 0.3 was reached. Isopropyl β-D-1-thiogalactopyranoside (IPTG) was added to a final concentration of 0.5 mM, and the growth temperature was reduced to 25 °C. The cells were then allowed to grow for 20 h before being collected via centrifugation. Cell lysis was performed as described previously (*13*) except that the cleared lysate was incubated with ~100 mg of hemin chloride dissolved in 1 mL of 0.2 M NaOH for 8 h with stirring at 4 °C. The protein was purified using affinity and ion-exchange chromatography as described elsewhere (*13*).

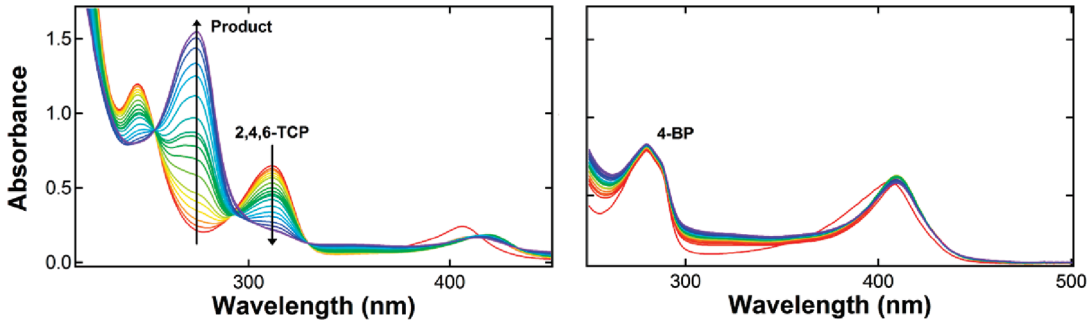

FIGURE 2: UV−vis enzymatic assay illustrating 2,4,6-TCP and 4-BP activity. The differences in activity between 2,4,6-TCP (left) and 4-BP (right) are shown. The figures represent a 600 s assay going from red (0 s) to blue (600 s). The 2,4,6-TCP molecule is completely converted to product 2,6-dichloro-1,4-benzoquinone (left) while the 4-BP molecule does not experience turnover (right).

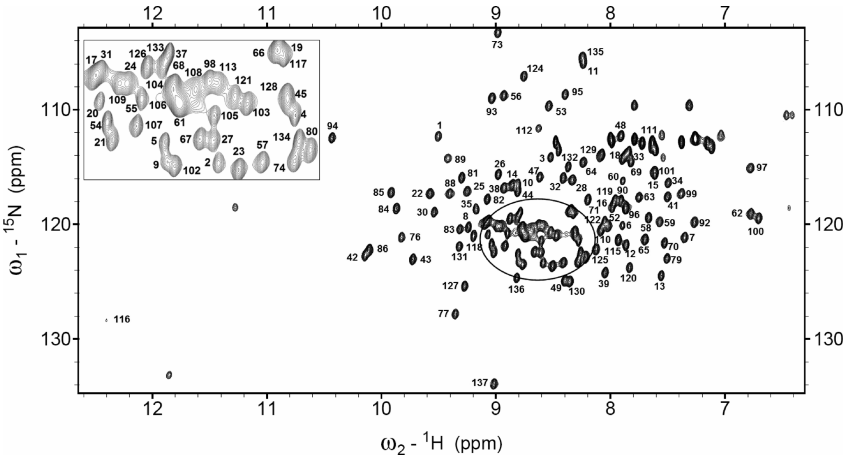

FIGURE 3: $^{1}H-^{15}N$ HSQC of DHPCN A collected at 298 K. The $^{1}H-^{15}N$ HSQC shows minimal overlap, and the crowded area of the spectrum (circled region) is shown in the inset for clarity. Backbone amide ^{1}H resonances are labeled.

Final yields of $^{13}C/^{15}N$-labeled DHP A were 24.5 mg/L using this protocol with A_{406}/A_{280} ratios greater than 4.

Sample Preparation and NMR Spectroscopy. All NMR samples were prepared using 90% H_2O/10% D_2O and 100 mM potassium phosphate buffer, pH 7. The protein was concentrated to 1.6 mM for all 3D NMR experiments, and KCN was added between 5× and 10× excess. All NMR experiments were collected on a Varian Inova 600 MHz spectrometer equipped with a Varian cryogenic $^{1}H/^{13}C/^{15}N$ triple resonance probe. For the 4-BP and 2,4,6-TFP titrations, a $^{1}H-^{15}N$ HSQC experiment was collected at 0:1, 1:1, 2:1, 3:1, 4:1, 5:1, 6:1, 7:1, 10:1, 12:1, and 15:1 halophenol to protein ratios. Only ratios of 0:1, 1:1, 2:1, 3:1, and 4:1 were feasible for the 2,4,6-TCP titration due to its poor water solubility. All NMR experiments were conducted at 298 K, processed via NMRPipe (*24*), and analyzed using Sparky (*25*).

UV−Vis Enzymatic Assays. For all experiments DHP A was oxidized via addition of excess $K_3Fe(CN)_6$. The excess ferricyanide was removed, and DHP A was buffer exchanged into 100 mM potassium phosphate, pH 7, using a Sephadex G-25 column. All absorption data were collected on a Hewlett-Packard 8453 multiwavelength spectrometer. Spectra were collected every 5 s over a 600 s time frame. The conditions used for the assays were ~2.5 μM DHP A, 120 μM H_2O_2, and 120 μM substrate or inhibitor. Turnover of the halophenols was determined by the disappearance of its respective absorption bands at pH 7 (4-BP, 280 nm; 2,4,6-TCP, 313 nm) and appearance of product absorption bands (2,6-dichloro-1,4-benzoquinone (2,6-DCQ), 272 nm).

RESULTS

Figure 2 illustrates the differences in activity between the monohalogenated 4-BP and trihalogenated 2,4,6-TCP. Upon addition of H_2O_2, complete conversion of 2,4,6-TCP to 2,6-DCQ is observed over the course of the assay (red = 0 s; blue = 600 s). The oxidation of 2,4,6-TCP can be seen by the decrease in absorption at 313 nm and the concomitant appearance of the 2,6-DCP product band at 273 nm. 4-BP, on the other hand, has been shown to be an efficient inhibitor of DHP A activity (*15*). Upon addition of H_2O_2 the 4-BP absorption band at 280 nm is not diminished, and during the 600s assay no detectable product band is observed.

Using $^{15}N-^{1}H$ HSQC, HNCO, HCACOCANH, HNCOCA, HNCA, and HNCACB, ~92% of the backbone $^{13}C\alpha$, $^{13}C\beta$, carbonyl ^{13}C, amide ^{1}H, and ^{15}N resonances were assigned in metcyano DHP A. The quality of the $^{15}N-^{1}H$ HSQC spectrum (Figure 3) shows good peak dispersion with minimal peak overlap, indicating a well-folded stable protein. The inset shows the crowded region between 9.2 and 8.2 ppm (^{1}H) for clarity. The cross-peaks at 11.8 (^{1}H), 133.0 ppm (^{15}N) and 11.2 (^{1}H), 118.5 ppm (^{15}N) arise from the nonbackbone W120 NεH and H55 NεH side chain resonances, respectively. DHP A contains one Trp (W120) and two His residues (H89, H55). The two His residues are the conserved proximal (H89) and distal (H55) histidines and are both susceptible to the paramagnetic effects of the CN-ligated heme iron. The exchangeable NεH of H89 exhibits considerable hyperfine shifting and was assigned in our previous work at 19.9 ppm (^{1}H) (*13*). In the ^{1}H NMR spectrum of

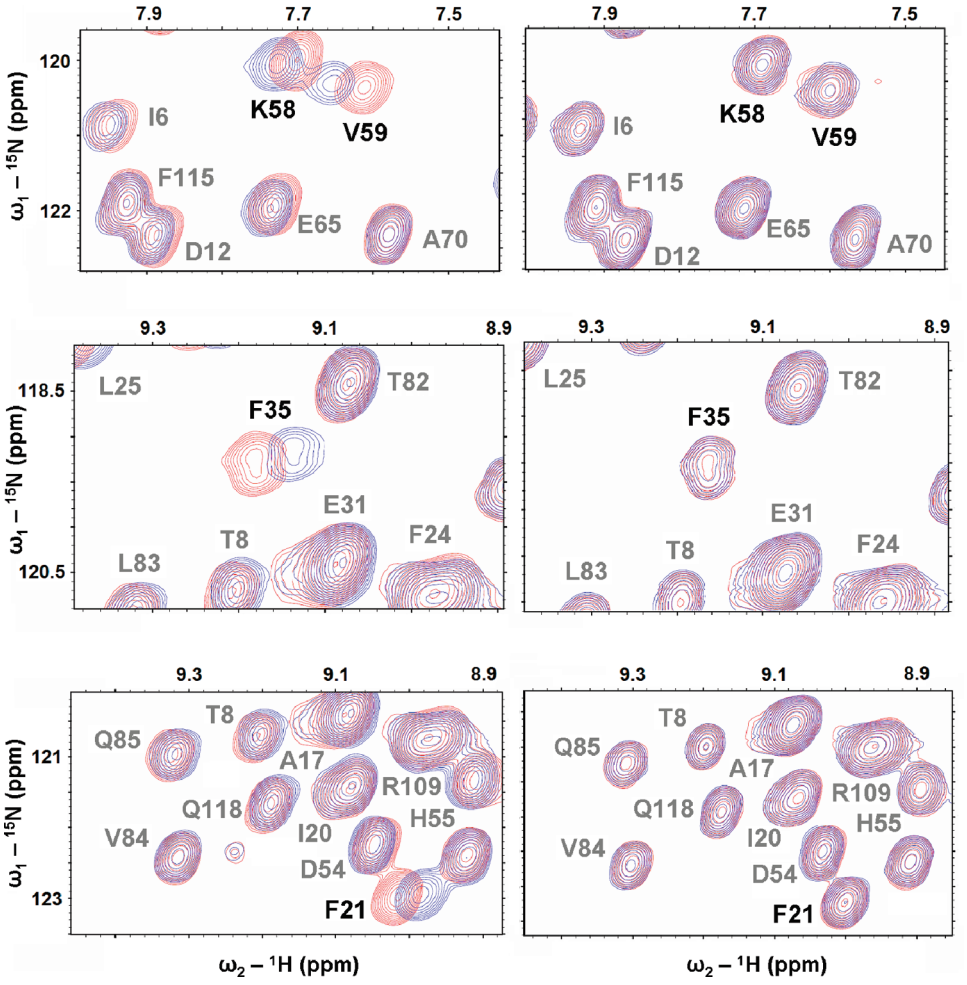

FIGURE 4: $^{1}H-^{15}N$ HSQC of DHPCN A titrated with 4-BP (left column) and 2,4,6-TCP (right column). The amide ^{1}H resonances which exhibit the greatest change in chemical shift upon addition of 4-BP are shown. Upon addition of 2,4,6-TCP these same resonances show no observable deviations.

a H55 V mutant, the hyperfine-shifted exchangeable at 11.2 ppm (H55 NεH) disappears while the other exchangeable at 11.8 ppm (W120 NεH) remains unchanged, confirming assignment of these resonances.

Amide proton chemical shift deviations upon introduction of inhibitor 4-BP and substrates 2,4,6-TCP and 2,4,6-TFP were quantified (eq 1) via a weighted chemical shift formula to account for the difference in backbone peak dispersion in the ^{15}N and ^{1}H dimensions (8.29-fold difference) (*26*, *27*).

$$\Delta\delta\ (\text{ppm}) = \sqrt{(^{1}\text{H}\ \delta\ (\text{ppm}))^2 + \frac{(^{15}\text{N}\ \delta\ (\text{ppm}))^2}{8.29}} \qquad (1)$$

Residues F60, F35, K99, R122, and V59 respectively represent the five largest deviations and V128, S42, G1, F21, and K58 respectively experience the next largest chemical shift alterations in the presence of 4-BP. Three of the top five (and five of the top ten) deviations occur in residues comprising the hydrophobic internal distal binding pocket: F21, F35, K58, V59, and F60. Current X-ray structures indicate that F35, V59, and F21 are the closest residues to bound 4-iodophenol (4-IP) having respective C−C distances of 2.98, 2.98, and 3.41 Å (*14*). The panels on the left in Figure 4 show these deviations in the presence of inhibitor 4-BP, while the panels on the right show responses of these same resonances upon addition of substrate 2,4,6-TCP. A large disparity was seen in the effects these two molecules had on the internal binding pocket, as no changes in chemical shift were observed in this local area upon addition of substrate 2,4,6-TCP. In addition to deviations in the distal pocket, 4-BP also induces changes in the local area near the dimer interface. These include perturbations of R122 and G1. Together, the internal binding pocket and dimer interface comprise 80% of the ten largest chemical shift changes in the presence of 4-BP.

The largest chemical shift deviations induced by the substrate 2,4,6-TCP occur in regions distinct from the internal binding pocket. The R122 amide proton and exchangeable side chain H55 NεH proton experience the largest degree of change in the presence of substrate 2,4,6-TCP. G1, S129, L76, Y34, E45, L100, D116, and N126 respectively experience the next eight largest chemical shift alterations when 2,4,6-TCP is titrated in. Some of the greatest deviations in the presence of 2,4,6-TCP can be observed in Figure 5. With the exception of the distal H55 NεH, the average weighted chemical shift deviation for 2,4,6-TCP was 11% lower than that of 4-BP. This may be attributed to the relatively low water solubility of the halophenols, as this permitted only a 4× excess of 2,4,6-TCP versus a 15× excess of 4-BP. 2,4,6-TFP was the only trihalogenated substrate soluble enough to reach a 15× excess concentration. While the smaller 2,4,6-TFP molecule is an active substrate, it is not as active as others such as 2,4,6-TCP or 2,4,6-TBP (*13*, *28*). With the addition of 2,4,6-TFP the greatest changes in chemical shift were observed in K99, Q4, H55 NεH, G1, M108, W120 NεH, L100, F60, F35, and E45, respectively (see Supporting Information). At a

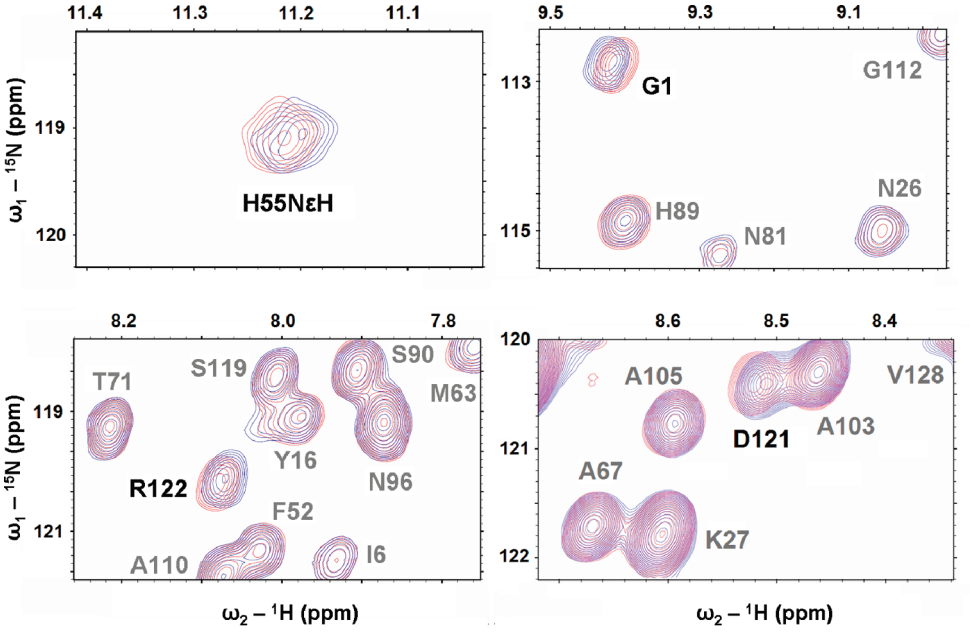

FIGURE 5: $^{1}H-^{15}N$ HSQC spectrum of DHPCN A titrated with 2,4,6-TCP. The amide ^{1}H resonances exhibiting some of the largest deviations are shown. These include the exchangeable distal histidine H55 NεH and amide protons of G1, R122, and D121.

15× excess of 2,4,6-TFP, the average chemical shift deviation was the lowest of the halophenols studied (72% lower than that of 4-BP). 2,4,6-TFP is believed to be the weakest binding trihalogenated phenol. In the monohalogenated phenol series, replacement of the chlorine substituent with a fluorine atom results in an increase in K_D from 1.7 to 3.7 mM (*15*). It is unclear if this decrease in binding affinity translates to the trihalogenated series. This assumption justifies the significantly lowered chemical shift deviations observed with 2,4,6-TFP.

DISCUSSION

The NMR backbone data presented here support the hypothesis that substrate and inhibitor have distinct binding sites in DHP A. The large effect of 4-bromophenol on binding pocket residues F21, F35, K58, V59, and F60 is consistent with internalization of the inhibitor in the distal pocket. The initial proposal that the internal site was the substrate binding site was reasonable on the grounds that such a well-defined site would be assumed to have a function (*6*, *14*). However, it is now clear that the function of binding in this site is to inhibit catalysis by steric interference at the heme iron (*15*). Steric interference both decreases the binding affinity of H_2O_2 at the heme iron and removes the acid−base catalyst, H55, from the distal pocket.

In order to extract structural information from the NMR data, the chemical shift perturbations caused by 4-BP, 2,4,6-TCP, and 2,4,6-TFP have been mapped onto the 2QFK X-ray structure of the protein (Figure 6) (*5*). The five largest deviations for each halophenol are shown in red, while the next five largest are shown in blue. The heme and W120 side chain are displayed in black. The heme and W120 sites serve as focal points for substrate binding analysis, because both are capable of retaining a reactive radical species necessary for the oxidation of 2,4,6-TCP or 2,4,6-TFP (*29*, *30*). The top panel in Figure 6 illustrates the effects of 4-BP addition. With the exception of R122, the most prominent changes (red) surround the internal binding pocket. The internal binding pocket residues F21, F35, K58, V59, and F60 exhibit large chemical shift deviations. However, it is not immediately apparent why residues near the dimer interface (R122 and G1) also exhibit significant perturbations. This could indicate either an allosteric effect or nonspecific binding interactions at the interface. Given the correlation between existing X-ray data and current $^{1}H-^{15}N$ HSQC data, there is little doubt regarding the

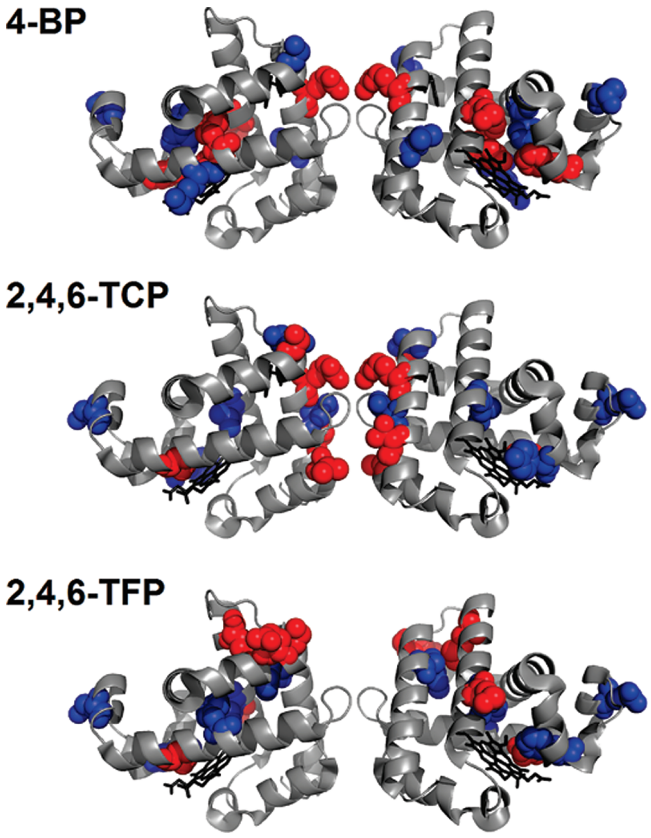

FIGURE 6: The residues experiencing the largest chemical shift deviations have been mapped onto the 2QFK X-ray structure (*5*). The side chains in red represent the five largest chemical shift changes, and the residues in blue represent the next five largest deviations. The heme and W120 residue (black) are provided as focal points. The panels display the largest deviations caused by addition of 4-BP, 2,4,6-TCP, and 2,4,6-TFP, respectively.

internalization of inhibitor 4-BP. However, since it has not been possible to obtain an X-ray structure of the bound substrate, and evidence points to an external site, $^{1}H-^{15}N$ HSQC data are one of the few current measurements that can be used to locate the binding site of substrates 2,4,6-TCP and 2,4,6-TFP under ambient conditions.

As can seen in Figure 4, in contrast to 4-BP, the internal pocket resonances do not exhibit a noticeable difference when titrated with the substrate 2,4,6-TCP. Instead, the local area surrounding the dimer interface shows four out of the five largest chemical shift perturbations (Figure 6). Of the five largest changes (R122, H55 NεH, G1, S129, and L76, respectively) only the distal histidine, H55 NεH, is not located near the interface. This result is surprising given the distal histidine is separated from the dimer interface by a distance of nearly 25 Å (*5*). Binding of substrate 2,4,6-TFP has aspects of contributions seen in both 4-BP and 2,4,6-TCP. As observed in Figure 6, alterations in chemical shift occurred near the internal pocket (F35, H55 NεH, and F60) and at a surface-exposed tryptophan near the interface (G1, Q4, M108, and W120). Previous NMR studies showed that internal heme substituents (most notably the 3-CH_3 heme methyl) were not affected by addition of 2,4,6-TFP but showed significant changes in the presence of 4-BP. These data indicate that the larger 4-BP has a much more pronounced effect in the distal pocket than 2,4,6-TFP (*13*). Thus, 2,4,6-TFP has some access to the distal pocket, but significantly less than 4-BP (*13*) and by extension other 4-halophenols (*15*). On the basis of these data we hypothesize that 2,4,6-TFP may act as both a substrate and a weakly bound inhibitor, which would explain the decreased activity of 2,4,6-TFP compared to 2,4,6-TCP (*13*, *28*).

The disparity in perturbations caused by monohalogenated inhibitor versus trihalogenated substrate indicates the importance of the 2- and 6-positions of the phenol in determining the binding site. In this study, the monohalogenated inhibitor primarily affects the internal distal pocket, while both trihalogenated substrates create perturbations externally near the heme edge (H55) and dimer interface region near W120. The presence of 2- and 6-position substituents on the phenol ring appears to be a decisive factor in controlling substrate and inhibitor binding locations. Steric and/or electrostatic effects of halogens at the 2- and 6-positions likely restrict substrate access to the internal distal binding pocket. While both substrates (2,4,6-TCP and 2,4,6-TFP) have a significant effect on the distal H55, both differ slightly in the perturbations induced near the dimer interface region (Figure 6, red spheres). Binding of the smaller 2,4,6-TFP substrate creates more localized deviations near W120, while 2,4,6-TCP binding appears to have a greater influence at the dimer interface. It is possible that the substrate binding site involves specific interactions with the halogens, and native 2,4,6-TBP may bind even more tightly than 2,4,6-TCP or 2,4,6-TFP. However, the low solubility of 2,4,6-TBP renders direct comparison impossible. Indeed, similar size dependencies were recently observed in various X-ray structures of bound monohalogenated phenol in the distal pocket (*15*). It was found that smaller monohalogated phenols (4-fluorophenol and 4-chlorophenol) bind with lower affinities and do not penetrate the internal pocket as efficiently when compared to larger monohalogenated phenols (4-bromophenol and 4-iodophenol).

In general, the NMR data indicate that binding of substrate may involve one of two possible scenarios. First, binding of the substrate may occur primarily on the external edge of the distal histidine, H55. This conclusion is reached on the basis that the second highest chemical shift change in 2,4,6-TCP, and third largest in 2,4,6-TFP, occurs at the distal H55 NεH. Earlier FT-IR experiments on the isoelectric, ferrous DHPCO A adduct indicated the orientation of H55 was in the "closed" conformation at pH 7, 290 K (*12*). If H55 is in the closed conformation, then the observed deviations of H55 NεH are likely the result of a perturbation in the Nε-H···NC hydrogen bond, where NC refers to bound cyanide. The lack of internal pocket deviations upon 2,4,6-TCP addition rules out binding of the molecule on the internal side of H55 (i.e., the distal 4-BP binding pocket). Binding of the molecule on the solvent-exposed, external side of H55 could be the cause for the deviation in the H55 NεH chemical shift. This scenario would place the substrate near the heme edge in an external fashion which is typical of other heme peroxidases, such as HRP. Peroxidases like HRP commonly perform substrate oxidation at the heme in an edge-on conformation (*29*). In addition, recent resonance Raman data on metaquo DHP A indicate an increase in 6-coordinate heme upon addition of 2,4,6-TCP consistent with a "push" of H55 toward the protein interior, adding credence to this mode of binding (*15*). There is also a long-standing precedent for allosteric changes at dimer interfaces as a result of axial ligand perturbations. Although cooperative binding and allosteric changes are typically related to tetrameric Hbs, many well-known studies have illustrated similar changes in more primitive, dimeric Hbs such as DHP A (*31*−*33*). Alterations in H55 NεH may affect the hydrogen bond between the H55 side chain and the axial ligand, ultimately resulting in allosteric communication via the dimer interface.

A second scenario involves direct binding of the substrate in the region near the interface. This scenario is highly plausible given the majority of residues with altered chemical shifts are located near a potentially redox-active tryptophan (W120). Upon inspection of the X-ray structures, this is the only residue in the interface area capable of acting as an oxidizing equivalent (i.e., a tryptophanyl radical). While the local shift deviations caused by 2,4,6-TCP appear evenly spread about the interface, the changes induced by 2,4,6-TFP are more localized near W120 (Figure 6). Many peroxidases, such as lignin peroxidase, manganese peroxidase, and versatile peroxidase, are known to bind and oxidize haloaromatics with high redox potentials near an exposed tryptophanyl radical (*34*−*36*). One of the most commonly studied peroxidases, cytochrome *c* peroxidase (CcP), is also known to generate a tryptophanyl radical (*37*). Upon addition of requisite cosubstrate H_2O_2, X-band EPR experiments do indicate the presence of a protein radical in DHP A that has tentatively been assigned as a tyrosyl radical (*22*). In fact, electronic similarities between the DHP A protein radical signature and the Trp191 radical species of CcP compound ES have led to naming this reactive intermediate "DHP A compound ES" (*22*). Although the EPR data reported for DHP A have been assigned to a tyrosyl radical when initially formed, analysis of the freeze-quenched radical signal at longer incubations times (> 12 s) led to the suggestion that the EPR signature could be a mixture of tyrosyl and tryptophanyl radicals (*22*). In structurally homologous sperm whale myglobin, there are three separate trappable protein radicals, including two tyrosyl (Y103 and Y151) and one tryptophanyl (W14) centered radical (*38*, *39*). In human hemoglobin up to four trappable radicals, including two tyrosyl (Y24 and Y42), one cysteinyl (C93), and one histidyl-based radical (H20), have been detected via the DMPO spin trap and subsequent MS analysis (*39*, *40*). Hence, there is precedent for formation of multiple protein radicals in structurally homolo-

gous globins, and there is no evidence that precludes the notion of radical hopping in DHP A. If tryptophanyl radical formation at W120 is a possibility, then a scenario involving 2,4,6-TCP or 2,4,6-TFP binding and oxidation near W120 should not be ruled out. Binding of the substrate at this site must however account for the change in H55 NεH. Because the heme edge and W120 are separated by nearly 9 Å, substrate binding near W120 must produce transferable long-range binding effects to the axial CN and likewise the H-bonded H55 NεH. Conducting enzymatic assays of various W120 mutants will help to determine any role W120 may have in substrate binding and overall protein activity.

The metcyano DHP adduct utilized in this study has been used previously to investigate halophenol binding interactions near the heme via 1D and 2D NMR experiments (*13*). Previous experiments demonstrated that DHPCN A exhibits a wide dispersion of chemical shifts (−12 to 27 ppm in the ^{1}H NMR spectra), with resonances of the heme and nearby residues being hyperfine-shifted out from under the diamagnetic envelope. The hyperfine shifts are due to a combination of contact, pseudocontact, and dipolar shift contributions arising from the $S = {}^1/_2$ paramagnetic heme center (*41*). Several resonances of nonligated residues experiencing large hyperfine shifts (i.e., proximal side F97 Cζ, Cε, and Cδ ring protons) were found to *lack* broadening and/or chemical shift deviations in the presence of substrate 2,4,6-TFP. This is significant as variations in dipolar contributions to the overall chemical shift are highly dependent on the orientation of the magnetic susceptibility tensor, χ, which is directly correlated to the Fe−CN tilt angle, β, from the heme normal (*42*−*44*). Chemical shift deviations in hyperfine-shifted resonances of nonligated residues, such as F97, would be expected if substrate binding induced structural rearrangements at or near the residue or if substrate binding altered the relative Fe−CN tilt angle, β. The Fe−CN tilt angle does not appear to be altered in the presence of active substrates like 2,4,6-TFP and suggests that chemical shift deviations observed in the distal H55NεH are not due to slight changes in the dipolar field. This rationale is supported by the lack of chemical shift deviations in other strongly paramagnetically influenced resonances, such as F97 CδHs, CεHs, and CζH and H89 Cβ Hs (*13*).

Deviations in the Fe−CN tilt angle cannot, however, be ruled out in the presence of inhibitor 4-BP. Previously reported NMR data indicated that resonances with large dipolar shifts (e.g., F97 ring protons) experience broadening and chemical shift deviations upon titration of 4-BP and not 2,4,6-TFP (*13*). Data from the current ^{1}H−^{15}N HSQC experiments indicate titration of 4-BP primarily results in alterations of *distal* side amide protons. In a previous report it was not fully understood why the ring protons of F97, a residue on the *proximal* side of the 3-CH_3 heme methyl, had such a sensitive response to the presence of 4-BP. One possible explanation could lie in a slight alteration of the Fe−CN tilt angle induced by steric interactions with inhibitor 4-BP in the distal pocket. This explanation is logical since NMR (*vide supra*) and X-ray data now indicate 4-BP bound in the distal pocket less than 4 Å from the heme iron (*14*, *15*).

CONCLUSION

The NMR study shows a distinct difference in the binding interactions of a 4-halophenol inhibitor and 2,4,6-trihalogenated phenol substrates. Binding of a 4-halophenol inhibitor, 4-BP, produced the greatest deviations in backbone chemical shifts in the distal binding pocket. Addition of trihalogenated substrate 2,4,6-TCP resulted in deviations largest at the distal H55 NεH and dimer interface. No significant changes were observed in internal binding pocket resonances upon addition of 2,4,6-TCP, clearly illustrating that binding of substrate 2,4,6-TCP is substantially different and separate from that of inhibitor 4-BP. Introduction of the smaller 2,4,6-TFP substrate showed a combination of the chemical shift changes observed for 4-BP and 2,4,6-TCP. These deviations include alterations at the internal pocket and surface tryptophan (W120) near the interface. Two scenarios were presented that may tie together the activity of 2,4,6-TCP and its observed binding perturbations. First, binding of the substrate on the external side of H55 could create allosteric changes at the dimer interface. This is in agreement with long-standing precedents relating allosteric changes at dimer interfaces to axial ligand perturbations. A second scenario involves direct binding near W120 itself. In both cases, the substrate molecule would be in favorable position for oxidation either along the heme edge or at a potential tryptophanyl radical, respectively. The NMR results have provided crucial insight into binding interactions between the protein and a highly active substrate, 2,4,6-TCP. Increased knowledge of the substrate binding site in DHP A will provide an understanding into toxic haloaromatic binding events in this bifunctional hemoglobin and possibly increase the opportunity to use DHP A for bioremediation processes beyond its native function that involves oxidation of 2,4,6-TBP.

SUPPORTING INFORMATION AVAILABLE

Full backbone chemical shift assignments and ^{1}H−^{15}N HSQC data upon titration of 2,4,6-TFP. This material is available free of charge via the Internet at http://pubs.acs.org.

REFERENCES

1. Han, K. P., Woodin, S. A., Lincoln, D. E., Fielman, K. T., and Ely, B. (2001) *Amphitrite ornata*, a marine worm, contains two dehaloperoxidase genes. *Mar. Biotechnol. 3*, 287–292.
2. de Serrano, V., D'Antonio, J., Thompson, M. K., Franzen, S., and Ghiladi, R. A. (2010) Crystal structure of dehaloperoxidase B at 1.58 Å and structural characterization of the A/B dimer from *Amphitrite ornata*, J. Biol. Chem. (submitted for publication).
3. D'Antonio, J., D'Antonio, E. L., Bowden, E. F., Smirnova, T. S., Franzen, S. F., and Ghiladi, R. A. (2010) Spectroscopic and mechanistic investigations of dehaloperoxidase B from *Amphitrite ornata*, J. Biol. Chem. (submitted for publication).
4. Chen, Z., De Serrano, V., Betts, L., and Franzen, S. (2009) Distal histidine conformational flexibility in dehaloperoxidase from *Amphitrite ornata*. *Acta Crystallogr., Sect. D: Biol. Crystallogr. 65*, 34–40.
5. de Serrano, V., Chen, Z. X., Davis, M. F., and Franzen, S. (2007) X-ray crystal structural analysis of the binding site in the ferric and oxyferrous forms of the recombinant heme dehaloperoxidase cloned from *Amphitrite ornata*. *Acta Crystallogr., Sect. D: Biol. Crystallogr. 63*, 1094–1101.
6. Lebioda, L., LaCount, M. W., Zhang, E., Chen, Y. P., Han, K., Whitton, M. M., Lincoln, D. E., and Woodin, S. A. (1999) An enzymatic globin from a marine worm. *Nature 401*, 445.
7. Weber, R. E., Mnum, C. P., Steinman, H., Bonaventura, C., Sullivan, B., and Bonaventura, J. (1977) Hemoglobins of two terebellid polychaetes: *Enoplobranchus sanuigneus* and *Amphitire ornata*. *Comp. Biochem. Physiol. 56A*, 179–187.
8. Belyea, J., Gilvey, L. B., Davis, M. F., Godek, M., Sit, T. L., Lommel, S. A., and Franzen, S. (2005) Enzyme function of the globin dehaloperoxidase from *Amphitrite ornata* is activated by substrate binding. *Biochemistry 44*, 15637–15644.
9. Franzen, S., Gilvey, L. B., and Belyea, J. L. (2007) The pH dependence of the activity of dehaloperoxidase from *Amphitrite ornata*. *Biochim. Biophys. Acta 1774*, 121–130.
10. Franzen, S., Chaudhary, C., Belyea, J., Gilvey, L., Davis, M. F., Sit, T. L., and Lommel, S. A. (2006) Proximal cavity, distal histidine and substrate hydrogen-bonding mutations modulate the acti-

vity of *Amphitrite ornata* dehaloperoxidase. *Biochemistry 45*, 9085–9094.
11. Nienhaus, K., Nickel, E., Davis, M. F., Franzen, S., and Nienhaus, G. U. (2008) Determinants of substrate internalization in the distal pocket of dehaloperoxidase hemoglobin of *Amphitrite ornata*. *Biochemistry 47*, 12985–12994.
12. Nienhaus, K., Deng, P. C., Belyea, J., Franzen, S., and Nienhaus, G. U. (2006) Spectroscopic study of substrate binding to the carbonmonoxy form of dehaloperoxidase from *Amphitrite ornata*. *J. Phys. Chem. B 110*, 13264–13276.
13. Davis, M. F., Gracz, H., Vendeix, F. A. P., de Serrano, V., Somasundaram, A., Decatur, S. M., and Franzen, S. (2009) Different modes of binding of mono-, di- and trihalogenated phenols to the hemoglobin dehaloperoxidase from *Amphitrite ornata*. *Biochemistry 48*, 2164–2172.
14. Zhang, E., Chen, Y. P., Roach, M. P., Lincoln, D. E., Lovell, C. R., Woodin, S. A., Dawson, J. H., and Lebioda, L. (1996) Crystallization and initial spectroscopic characterization of the heme-containing dehaloperoxidase from the marine polychaete *Amphitrite ornata*. *Acta Crystallogr., Sect. D 52*, 1191–1193.
15. Nicoletti, F. P., Thompson, M. K., Howes, B. D., Franzen, S., and Smulevich, G. (2010) New Insights into the Role of Distal Histidine Flexibility in Ligand Stabilization of Dehaloperoxidase-hemoglobin from *Amphitrite ornata*. *Biochemistry* (DOI: 10.1021/bi9020567).
16. Shikama, K. (2006) Nature of the FeO_2 bonding in myoglobin and hemoglobin: A new molecular paradigm. *Prog. Biophys. Mol. Biol. 91*, 83–162.
17. Fielman, K. T., Woodin, S. A., and Lincoln, D. E. (2001) Polychaete indicator species as a source of natural halogenated organic compounds in marine sediments. *Environ. Toxicol. Chem. 20*, 738–747.
18. Fielman, K. T., Woodin, S. A., Walla, M. D., and Lincoln, D. E. (1999) Widespread occurrence of natural halogenated organics among temperate marine infauna. *Mar. Ecol.: Prog. Ser. 181*, 1–12.
19. Woodin, S. A., Lindsay, S. M., and Lincoln, D. E. (1997) Biogenic bromophenols as negative recruitment cues. *Mar. Ecol.: Prog. Ser. 157*, 303–306.
20. Lincoln, D. E., Fielman, K. T., Marinelli, R. L., and Woodin, S. A. (2005) Bromophenol accumulation and sediment contamination by the marine annelids *Notomastus lobatus* and *Thelepus crispus*. *Biochem. Systemat. Ecol. 33*, 559–570.
21. Osborne, R. L., Taylor, L. O., Han, K. P., Ely, B., and Dawson, J. H. (2004) *Amphitrite ornata* dehaloperoxidase: Enhanced activity for the catalytically active globin using MCPBA. *Biochem. Biophys. Res. Commun. 324*, 1194–1198.
22. Feducia, J., Dumarieh, R., Gilvey, L. B. G., Smirnova, T., Franzen, S., and Ghiladi, R. A. (2009) Characterization of dehaloperoxidase compound ES and its reactivity with trihalophenols. *Biochemistry 48*, 995–1005.
23. Smirnova, T. I., Weber, R. T., Davis, M. F., and Franzen, S. (2008) Substrate binding triggers a switch in the iron coordination in dehaloperoxidase from *Amphitrite ornata*: HYSCORE experiments. *J. Am. Chem. Soc. 130*, 2128–2129.
24. Delaglio, F., Grzesiek, S., Vuister, G. W., Zhu, G., Pfeifer, J., and Bax, A. (1995) NMRPipe: A multidimensional spectral processing system based on UNIX pipes. *J. Biomol. NMR 6*, 277–293.
25. Goddard, T. D., and Kneller, D. G. SPARKY 3, University of California, San Francisco.
26. Kordys, D. R., Bobay, B. G., Thompson, R. J., Venters, R. A., and Cavanah, J. (2007) Peptide binding proclivities of calcium loaded calbindin-D28k. *FEBS Lett. 581*, 4778–4782.
27. Palmer, S. M., Schaller, M. D., and Campbell, S. L. (2008) Vinculin tail conformation and self-association is independent of pH and H906 protonation. *Biochemistry 47*, 12467–12475.
28. Chaudhary, C. (2003) Functional studies of the push-pull mechanism in dehaloperoxidase from *Amphitrite ornata*, Master's Thesis, North Carolina State University.
29. Ator, M. A., and Ortiz de Montellano, P. R. (1987) Protein control of prosthetic heme reactivity: Reaction of substrates with the heme edge of horseradish peroxidase. *J. Biol. Chem. 262*, 1542–1551.
30. Pogni, R., Baratto, M. C., Giansanti, S., Teutloff, C., Verdin, J., Valderrama, B., Lendzian, F., Lubitz, W., Vazquez-Duhalt, R., and Basosi, R. (2005) Tryptophan-based radical in the catalytic mechanism of versatile peroxidase from *Bjerkandera adusta*. *Biochemistry 44*, 4267–4274.
31. Royer, W. E., Hendrickson, W. A., and Chiancone, E. (1990) Structural transitions upon ligand-binding in a cooperative dimeric hemoglobin. *Science 249*, 518–521.
32. Royer, W. E., Pardanani, A., Gibson, Q. H., Peterson, E. S., and Friedman, J. M. (1996) Ordered water molecules as key allosteric mediators in a cooperative dimeric hemoglobin. *Proc. Natl. Acad. Sci. U.S.A. 93*, 14526–14531.
33. Knapp, J. E., Bonham, M. A., Gibson, Q. H., Nichols, J. C., and Royer, W. E. (2005) Residue F4 plays a key role in modulating oxygen affinity and cooperativity in *Scapharca* dimeric hemoglobin. *Biochemistry 44*, 14419–14430.
34. Doyle, W. A., Blodig, W., Veitch, N. C., Piontek, K., and Smith, A. T. (1998) Two substrate interaction sites in lignin peroxidase revealed by site-directed mutagenesis. *Biochemistry 37*, 15097–15105.
35. Perez-Boada, M., Ruiz-Duenas, F. J., Pogni, R., Basosi, R., Choinowski, T., Martinez, M. J., Piontek, K., and Martinez, A. T. (2005) Versatile peroxidase oxidation of high redox potential aromatic compounds: Site-directed mutagenesis, spectroscopic and crystallographic investigation of three long-range electron transfer pathways. *J. Mol. Biol. 354*, 385–402.
36. Ruiz-Duenas, F. J., Pogni, R., Morales, M., Giansanti, S., Mate, M. J., Romero, A., Martinez, M. J., Basosi, R., and Martinez, A. T. (2009) Protein radicals in fungal versatile peroxidase: Catalytic tryptophan radical in both compound I and compound II and studies on W164Y, W164H, and W164S variants. *J. Biol. Chem. 284*, 7986–7994.
37. Sivaraja, M., Goodin, D. B., Smith, M., and Hoffman, B. M. (1989) Identification by ENDOR of Trp191 as the free-radical site in cytochrome-*c* peroxidase compound ES. *Science 245*, 738–740.
38. Gunther, M. R. (2004) Probing the free radicals formed in the metmyoglobin-hydrogen peroxide reaction. *Free Radical Biol. Med. 36*, 1345–1354.
39. Mason, R. P. (2004) Using anti-5,5-dimethyl-1-pyrroline *N*-oxide to detect protein radicals in time and space with immuno-spin trapping. *Free Radical Biol. Med. 36*, 1214–1223.
40. Bhattacharjee, S., Deterding, L. J., Jiang, J., Bonini, M. G., Tomer, K. B., Ramirez, D. C., and Mason, R. P. (2007) Electron transfer between a tyrosyl radical and a cysteine residue in hemoproteins: Spin trapping analysis. *J. Am. Chem. Soc. 129*, 13493–13501.
41. La Mar, G. N., and de Ropp, J. S. (1993) in Biological Magnetic Resonance, pp 1−73, Plenum Press, New York.
42. La Mar, G. N. (2007) Application of the paramagnetic dipole field for solution NMR active site structure determination in low-spin, cyanide-inhibited ferric hemoproteins. *IUBMB Life 59*, 513–527.
43. La Mar, G. N., Chen, Z., Vyas, K., and McPherson, A. D. (1995) An interpretive bases of the hyperfine shifts in cyanide-inhibited horseradish peroxidase based on the magnetic axes and ligand tilt. Influence of substrate binding and extensions to other peroxidases. *J. Am. Chem. Soc. 117*, 411–419.
44. Zhu, W., Li, Y., Wang, J., Ortiz de Montellano, P. R., and La Mar, G. N. (2006) Solution NMR study of environmental effects on substrate seating in human heme oxygenase: Influence of polypeptide truncation, substrate modification and axial ligand. *J. Inorg. Biochem. 100*, 97–107.